Dyes and Pigments 90 (2011) 239–244

Contents lists available at ScienceDirect

Dyes and Pigments

journal homepage: www.elsevier.com/locate/dyepig

Highly selective fluorescent and colorimetric sensor for Hg^{2+} based on triazole-linked NBD

Yi-Bin Ruan, Stéphane Maisonneuve, Juan Xie*

PPSM, Institut d'Alembert, ENS Cachan, CNRS, 61 av President Wilson, F-94230 Cachan, France

ARTICLE INFO

Article history:
Received 25 October 2010
Received in revised form
4 November 2011
Accepted 5 November 2011
Available online 13 January 2011

Keywords:
NBD
Triazole
Fluorescence
Naked-eye detection
Hg^{2+}

ABSTRACT

7-Nitrobenzo-2-oxa-1,3-diazole (NBD) derived compound **1** bearing triazole binding site was used as a selective fluorescent and colorimetric sensor for Hg^{2+} in aqueous solution. Among the metal ions examined, only Hg^{2+} caused significant fluorescence quenching in EtOH/HEPES (v/v = 9:1) at pH 7.4, along with a remarkable red shift in both absorption and fluorescence spectra which then facilitated naked-eye detection. ^1H NMR titration and control experiments by using more rigid triazolyl NBD derivative **2** were carried out to illustrate the complexation mode and the importance of cooperation of amino acid moiety and triazole ring in improving the binding ability of **1** to Hg^{2+}.

© 2011 Elsevier Ltd. All rights reserved.

1. Introduction

Contamination of mercury is a worldwide concern for decades due to its extreme toxicity, causing adverse effects on human health. Accumulation of mercury in vital organs and tissues may cause serious damages to the central nervous and endocrine systems [1]. Therefore great efforts have been devoted to the design of highly selective and sensitive chemosensors for detection of Hg^{2+} in recent years [2]. So far there have been several approaches based on organic fluorophores [3], DNAzyme [4], nanoparticles [5], protein [6] and conjugated polymers [7]. However, development of facile and practical chemosensors for Hg^{2+} is still a great challenge.

Cu(I)-catalyzed Huisgen 1,3-dipolar cycloaddition reaction between azide and alkyne is widely used as versatile tools in organic synthesis, medicinal chemistry, bioconjugated application and material chemistry [8]. Recently it was found that triazole could be a stabilizing ligand for coordination chemistry [9]. Incorporation with appropriate fluorophores, chemosensors based on triazole have been reported for various metal ions [10]. In our previous work, we have also reported selective detection of Zn^{2+}, Ni^{2+} and Cu^{2+} through precise introduction of triazole into various fluorophores [10n–r]. However, up to now there are still rare reports for the detection of mercury using triazole group as the binding sites, especially in aqueous solution [10a–c]. NBD derivatives have been widely used as fluorescent labeling reagents for their good spectral properties and cell permeability [11]. Furthermore, chemosensors based on NBD have been reported for various transition metal ions by virtue of ICT (intramolecular charge transfer) and PET (photo-induced electron transfer) processes [12]. As a continuous work on development of chemosensors for metal ions based on triazole coordination chemistry, compounds **1** and **2** containing NBD as signaling moiety and triazole as recognition moiety were used as double-channel fluorescent and colorimetric sensors for metal ions (Fig. 1). Meanwhile amino acid groups were integrated to investigate structure-dependent sensitivity.

2. Experimental section

2.1. Reagents and instruments

The tested metal salts included $Cu(ClO_4)_2$, $AgNO_3$, $Ba(ClO_4)_2$, $Mn(ClO_4)_2$, $Co(ClO_4)_2$, $Cd(ClO_4)_2$, $Zn(ClO_4)_2$, $Ni(ClO_4)_2$, $Fe(ClO_4)_2$, $Pb(ClO_4)_2$, $Mg(ClO_4)_2$, $Ca(ClO_4)_2$ and $Hg(ClO_4)_2$. Solvents of spectroscopic grade are purchased from SDS/Carlo Erba.

Absorption spectra were recorded on a Uvikon-940 KON-TRON spectrophotometer and corrected emission spectra were performed on a Jobin-Yvon Spex Fluorolog 1681 spectrofluorometer (1 cm quartz cell was used). The fluorescence quantum yield (Φ_F)

---

* Corresponding author. Tel.: +33 1 47405586; fax: +33 1 47402454.
E-mail address: joanne.xie@ppsm.ens-cachan.fr (J. Xie).

0143-7208/$ – see front matter © 2011 Elsevier Ltd. All rights reserved.
doi:10.1016/j.dyepig.2011.01.004

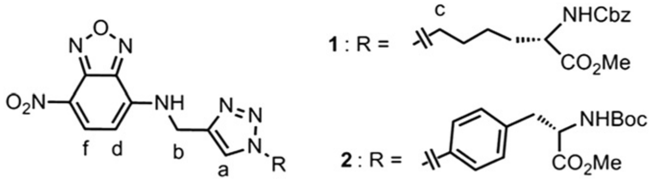

Fig. 1. Molecular structure of compounds **1** and **2**.

was determined by the standard method using coumarin 153 in ethanol as reference. The refractive index of the solvent was taken into account in the measurement. Fluorescence intensity decays were obtained by the single-photon timing method with picosecond laser excitation by use of a Spectra-Physics setup composed of a titanium sapphire Tsunami laser pumped by an argon ion laser, a pulse detector and doubling and tripling crystals. Data were analyzed by a nonlinear least-squares method with Globals software (Globals Unlimited, University of Illinois at Urbana-Champaign, Laboratory of Fluorescence Dynamics). NMR spectra were acquired on JEOL ECS400 spectrometer.

2.2. *Spectral measurement*

Stock solution of compounds **1** and **2** was prepared in DMSO while metal perchlorate salts in MeCN. HEPES buffered solutions with different pHs were adjusted with HNO_3 and NaOH. For all the spectral tests, concentrations of receptors were fixed at 10 μM. Before recording absorption and fluorescence spectra in aqueous solutions, the mixtures of receptor and metal ions were incubated for 7 min. ^1H NMR titration were tested in $CD_3OD/DMSO\text{-}d_6$ (4:1).

3. Results and discussion

3.1. *Photophysical properties of **1***

Compounds **1** and **2** can be easily synthesized by using Cu(I)-catalyzed Huisgen 1,3-dipolar azide-alkyne cycloaddition reaction which has been reported in our previous work [13]. As presented in Table 1, compound **1** in ethanol exhibits a characteristic absorption band centered at 456 nm ($\varepsilon = 19{,}858\ \mathrm{L\,mol^{-1}\,cm^{-1}}$) and emission band at 534 nm. This is assigned to ICT process from electron-donating amine group to electron-withdrawing nitro group, which generally could be judged from solvatochromic effect and broad structureless feature of the band. As shown in Fig. S1, a continuous red shift of the absorption band is observed with increasing polarity of solvents, from 447 nm in chloroform to 472 nm in DMSO. Fluorescence spectra of **1** show the similar solvent-dependent behavior which further indicates its ICT emissive state. Moreover, **1** shows high quantum yield up to 0.44 in ethanol which is quite different from the reported NBD derivatives with aminoethyl group directly linked to 4-N of NBD fluorophore [12]. This is due to the transformation of nitrogen hybridization form from sp^3 of amino group into sp^2 in triazole, which reduces the availability of the lone electron pair on nitrogen atom and suppresses the PET process. Fluorescence decay of **1** was also performed in EtOH. It consists of a long-lived major component (7.37 ns, 90%) and a short-lived minor component (2.9 ns, 10%). This illustrated that emission of **1** arises mainly from ICT process and short-lived component could be resulted from relatively weak PET from triazole ring to NBD fluorophore [12b]. The other photophysical parameters of **1** are collected in Table 1.

Table 1
Spectroscopic data of compounds **1** and **2**.

Compound	Solvent	λ^{A}_{max} [nm]	λ^{F}_{max} [nm]	$\Delta\lambda_{F\text{-}A}$ [nm]	ε_{00} [$\mathrm{L\,mol^{-1}\,cm^{-1}}$]	Φ_F	τ, ns
1	EtOH	456	534	78	19,858	0.44	7.37, 2.90
2	EtOH	456	534	78	19,858	0.46	–

3.2. *Spectral behavior of **1** to metal ions*

Considering the flexible coordination chemistry of triazole, we then first investigated fluorescence response of **1** to different metal ions such as Ag^+, Ba^{2+}, Ca^{2+}, Cd^{2+}, Co^{2+}, Cu^{2+}, Fe^{2+}, Hg^{2+}, Mn^{2+}, Mg^{2+}, Ni^{2+}, Pb^{2+} and Zn^{2+} in ethanol. As shown in Fig. S2, fluorescence intensity of **1** was quenched by Ag^+, Co^{2+}, Ni^{2+} and Hg^{2+} to different extents. Especially for Hg^{2+}, its quenching efficiency can be up to 80% and a remarkable red shift by 40 nm was observed. Other metal ions showed almost no influence. In view of the practical application of chemosensors, we then further tested the selectivity of **1** to different metal ions in EtOH/HEPES (v/v = 9:1) at pH 7.4. As displayed in Fig. 2, the selectivity has been greatly improved and only Hg^{2+} shows remarkable quenching effect while others display almost no influence even in large excess. This selectivity was further confirmed through study of the fluorescence behavior in the presence of a mixture of Hg^{2+} and other metal ions. As shown in Fig. S3, Fe^{2+} and Pb^{2+} do produce a little interference while other ions show almost no influence on the binding process of **1** to Hg^{2+}, which demonstrates the high selectivity of our approach for the detection of Hg^{2+}.

3.3. *Spectral titration of **1** to Hg^{2+}*

Fig. 3 shows the evolution of absorption spectra of **1** in the presence of varying [Hg^{2+}] in ethanol. With increasing [Hg^{2+}], the absorbance at 455 nm decreases while a new band appears at 493 nm. Such a red shift (38 nm) led to the solution color changing from light yellow to light orange. Three clear isosbestic points are observed at 467, 381 and 329 nm, which indicates the interconversion of spectral species in the presence of Hg^{2+}. Job plot experiment was then carried out to investigate the stoichiometry between Hg^{2+} and **1**. The results suggested 1:1 binding stoichiometry (Fig. S4). Nonlinear regression analysis of absorption titration then gave a large association constant up to $3.23 \times 10^6\ M^{-1}$ in the ground state. This may come from cooperative interactions of the multi-binding sites.

Fluorescence titration was also performed in ethanol, as shown in Fig. 4. Upon addition of increasing [Hg^{2+}], fluorescence intensity of **1** at 533 nm deceases gradually (50% quenched in the presence of 10 μM Hg^{2+}), concomitant with a red shift from 531 to 573 nm. Fluorescence titration was also analyzed by nonlinear regression based on 1:1 binding ratio, giving us the binding constant in the excited state to be $3.97 \times 10^6\ M^{-1}$, which is almost the same as that of ground state.

We then investigated the pH effect on the binding of **1** to Hg^{2+} in EtOH/HEPES (v/v = 9:1). As shown in Fig. 5, when pH value of the solution is lower than 7.4, decrease of pH suppresses the coordination interaction between **1** and Hg^{2+}. However, **1** works well in neutral or weakly basic conditions. Considering the practical application of chemosensors, titration of Hg^{2+} was further carried out in EtOH/HEPES (v/v = 9:1) at pH 7.4. As depicted in Figs. S5 and S6, both absorption and fluorescence titrations show the similar spectral behavior to that in EtOH. Nonlinear regression analysis shows that the association constants are dramatically reduced about one order magnitude which may be due to the conformation change and ionic solvation effect. However, a detection limit (S/N > 3) of 610 nM could be obtained for analyzing Hg^{2+} under the

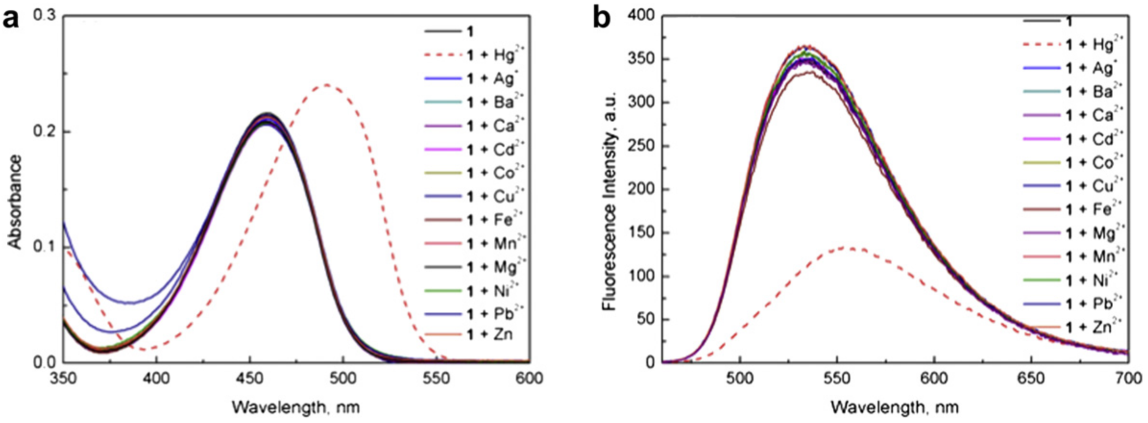

Fig. 2. Absorption (a) and fluorescence (b) spectra of **1** in the presence of different metal ions in EtOH/HEPES (v/v = 9:1) at pH 7.4. [**1**] = 10 μM, [Hg^{2+}] = 40 μM, [M^{n+}] = 200 μM, λ_{ex} = 456 nm.

above conditions. Finally, reversibility of our protocol could be easily realized by the addition of I^- (Fig. S7).

3.4. Naked-eye detection of Hg^{2+}

The remarkable wavelength shift both in the absorption and fluorescence spectra in the presence of Hg^{2+} promoted us to examine the selective naked-eye detection of Hg^{2+}. As shown in Fig. 6, only Hg^{2+} induces a color change from light yellow to light orange (Fig. 6a). And when excited under hand-UV lamp at 365 nm, fluorescence of **1** shows a color change from green to yellow (Fig. 6b). Furthermore, even in the coexistence of 20 equiv of other metal ions, only small influence has been detected with Fe^{2+} and Pb^{2+} (Fig. 6c,d).

3.5. Mechanism of the binding

In order to investigate effect of the terminal amino acid group on the binding ability towards metal ions, compound **2** with more rigid distal amino acid group was then examined. As shown in Table 1, compound **2** displays almost the same photophysical properties as that of **1**. Absorption and fluorescence titration were then carried out. Similar behaviors as that of **1** to Hg^{2+} were observed in absorption and fluorescence spectra (Figs. 7 and 8) and the results of job plot experiments (Fig. S8) also demonstrated 1:1 binding stoichiometry between **2** and Hg^{2+}. However, nonlinear regression analysis of the spectral titrations show that its binding constant with Hg^{2+} ($\sim 1 \times 10^5\ M^{-1}$) is one order magnitude lower than that of **1**, which might be explained by the participation of the flexible distal amino acid group of **1** in the complexation with Hg^{2+} and demonstrated the importance of Lys amino acid moiety in improvement of detection sensitivity. Therefore, incorporation of additional binding sites could be a new way for further work on the development of triazole chemistry for selective and sensitive molecular sensing applications.

To better understand the complexation mode of **1** to Hg^{2+}, ^1H NMR titration was then carried out in CD_3OD/DMSO-d_6 (1:1). As shown in Fig. 9, with increasing [Hg^{2+}], H_a on the triazole ring undergoes a remarkable downfield shift by 0.24 ppm from 8.01 to 8.25. Meanwhile, $C\underline{H}_b$ and $C\underline{H}_c$ linked to triazole ring shift downfield slightly. Furthermore, as shown in Fig. 10, when the assay is performed under acidic condition like pH 3.0, only 20% fluorescence quenching is observed immediately after the addition of 20 μM Hg^{2+} and then the spectra recover partially by itself within 15 min. As the spectral properties of **1** show no changes from pH 3.0 to 10.4 (Fig. S9), it illustrates that NBD fluorophore could not be protonated when pH is equal to 3.0. Therefore, the self-recovery of the fluorescence is due

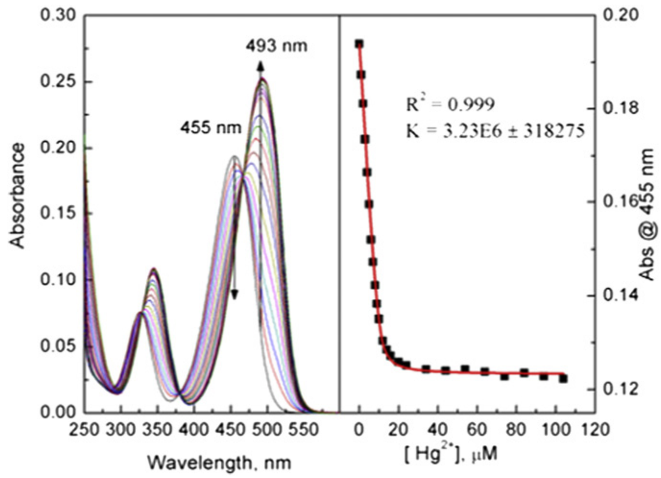

Fig. 3. Absorption spectra of **1** in the presence of varying concentrations of Hg^{2+} in ethanol and plot of absorbance of **1** at 455 nm as the function of [Hg^{2+}], [**1**] = 10 μM.

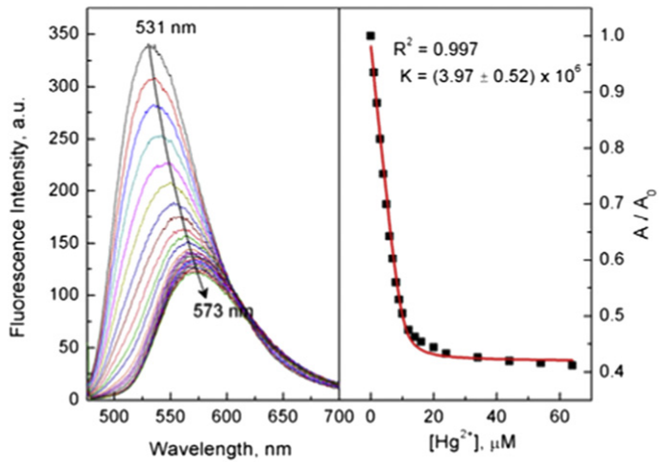

Fig. 4. Fluorescence spectra of **1** in the presence of varying concentrations of Hg^{2+} in ethanol and plot of fluorescence integral area of **1** as the function of [Hg^{2+}]; [**1**] = 10 μM, λ_{ex} = 476 nm.

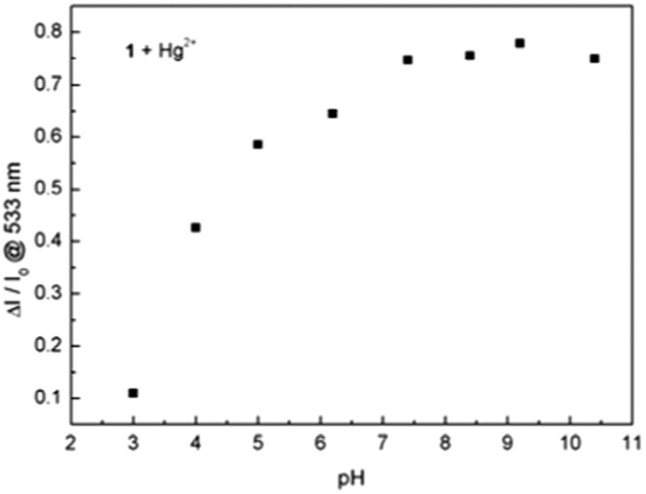

Fig. 5. Change of fluorescence intensity of **1** at 533 nm in the presence of Hg^{2+} in EtOH/HEPES (v/v = 9:1) under different pH conditions. [**1**] = 10 μM, [Hg^{2+}] = 40 μM, λ_{ex} = 459 nm, incubated time: 7 min and *I* indicate fluorescence intensity at 533 nm.

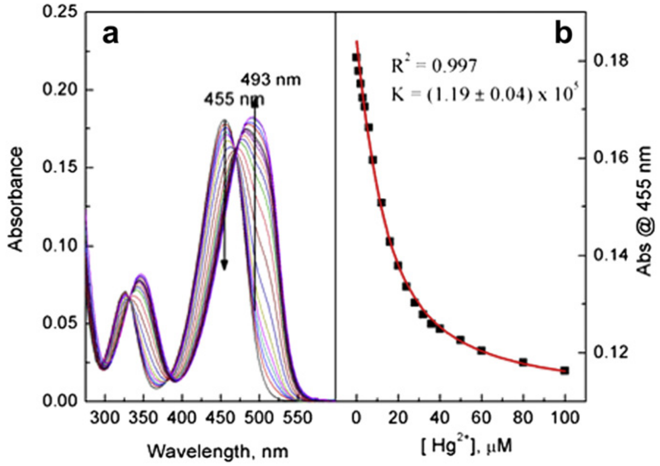

Fig. 7. (a) Absorption spectra of **2** in the presence of varying concentrations of Hg^{2+} in ethanol and (b) plot of absorbance of **2** at 455 nm as a function of [Hg^{2+}], [**2**] = 10 μM.

to the protonation of triazole moiety which suppresses the complexation of **1** to Hg^{2+}. These results clearly demonstrate that triazole group participates in the complexation with Hg^{2+}. However, these observations couldn't explain spectral behavior of **1** in the presence of Hg^{2+} because generally ICT process could not be affected through nonconjugated spacer. We then suppose that the complexation of Hg^{2+} to the NBD fluorophore could lead to red shift of the absorption and fluorescence spectra. Firstly, 4-NH might be a good candidate. If it binds to Hg^{2+} without deprotonation, reduction of the electron density of nitrogen atom would cause blue shift

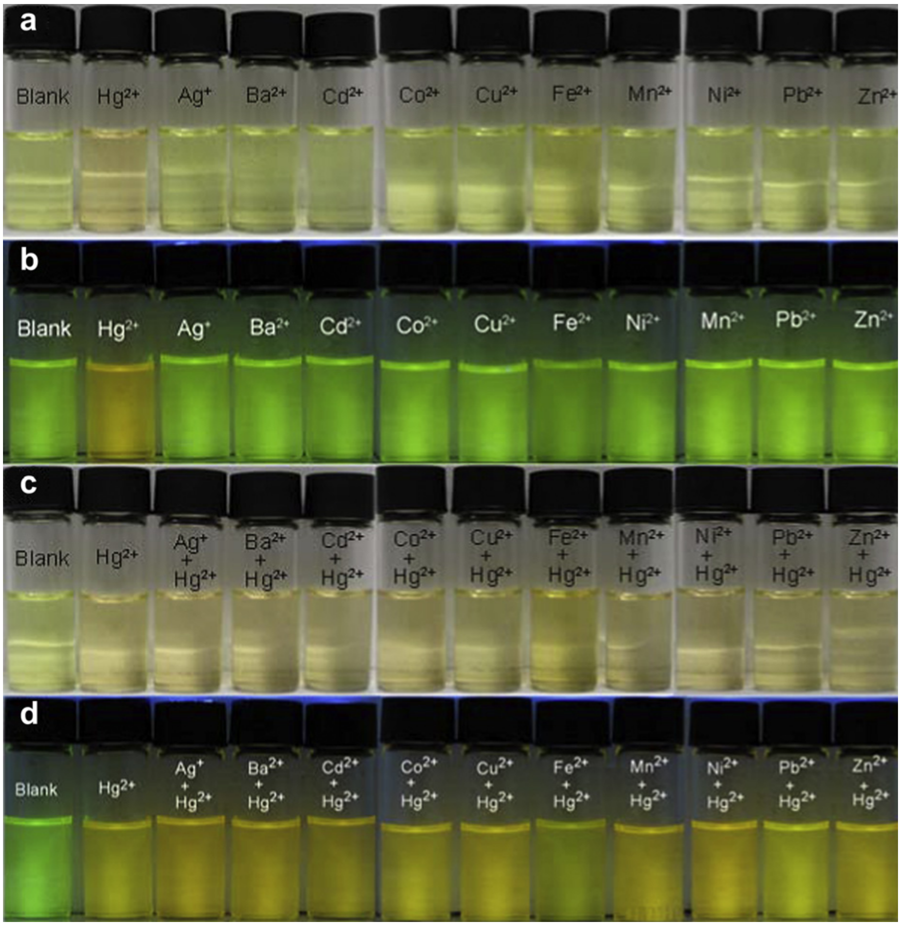

Fig. 6. Photographs of **1** in the presence of different metal cations (a) color, (b) fluorescence and coexistence of different kinds of metal ions and Hg^{2+} (c) color, (d) fluorescence in EtOH/HEPES (v/v = 9:1). [**1**] = 10 μM, [Hg^{2+}] = 40 μM, [M^{n+}] = 200 μM, illuminated under 365 nm.

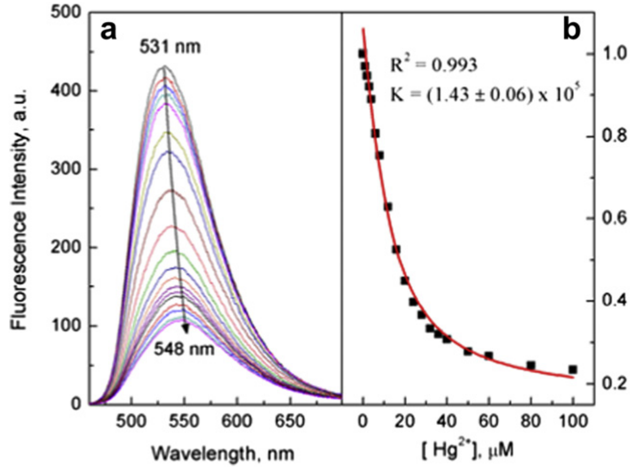

Fig. 8. (a) Fluorescence spectra of **2** in the presence of varying concentrations of Hg^{2+} in ethanol and (b) plot of fluorescence intensity of **2** at 533 nm as the function of $[Hg^{2+}]$, $[\mathbf{2}] = 10$ μM, $\lambda_{ex} = 455$ nm.

of the spectra; in contrast, if the addition of Hg^{2+} induces deprotonation of 4-NH, it will affect the chemical shift of $C\underline{H}_d$ and $C\underline{H}_f$. However, complexation of **1** with Hg^{2+} led to a remarkable red shift of the absorption band and no chemical shift of $C\underline{H}_d$ and $C\underline{H}_f$ was observed even in the presence of 2.0 equiv of Hg^{2+} (Fig. 9). These results demonstrate that 4-NH isn't the main binding site of **1** for Hg^{2+}. Samanta et al. have investigated spectral response of NAM (4-amino-7-nitrobenzo-2-oxa-1,3-diazole) to metal ions and attributed the spectral changes to the binding of metal ions with the NBD fluorophore [12b]. Worthy of notice is that no spectral shift was observed in the presence of metal ions. These results indicated that metal coordination of oxadiazole group in NBD could not induce spectral shift. Consequently, the possibility of coordination of NBD fluorophore to Hg^{2+} could be precluded. Finally, there exists another possibility because the mercury salt used in the experiment contains hydration shell. The binding of triazole moiety to hydrated Hg^{2+} might increase local polarity around the NBD fluorophore which result in remarkable red shift and fluorescence quenching. Therefore we can suppose that triazole and amino acid moiety in **1** together contribute to the complexation with Hg^{2+} and the resulting more polar microenvironment induces the related spectral changes. Our work is consistent with the reported results which demonstrate that triazole moiety, when coupled with some other weak binding site, could show highly selective binding ability to Hg^{2+} in appropriate protic solvents [10a].

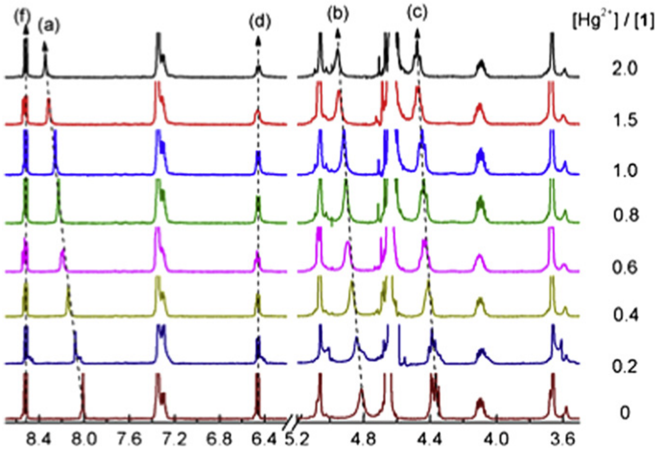

Fig. 9. Partial ^1H NMR spectra of **1** in the presence of varying concentrations of Hg^{2+} in CD_3OD/DMSO-d_6 (4:1).

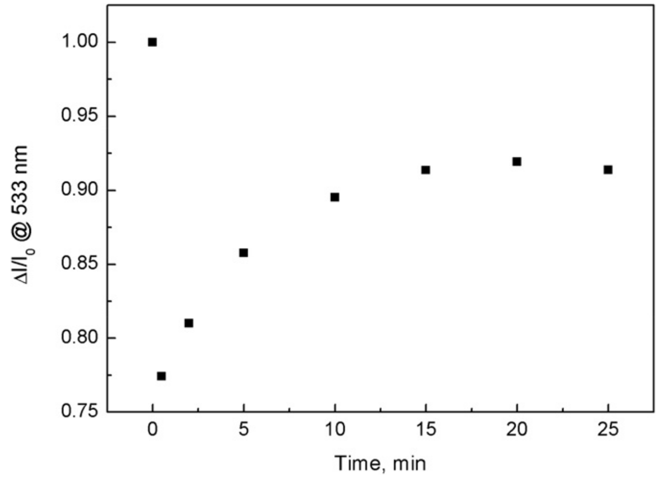

Fig. 10. Kinetics profiles of fluorescence intensity of **1** at 533 nm after addition of Hg^{2+} in EtOH/HEPES (v/v = 9:1) at pH 3.0; $[\mathbf{1}] = 10$ μM, $[Hg^{2+}] = 20$ μM, $\lambda_{ex} = 459$ nm and *I* indicate fluorescence intensity at 533 nm.

4. Conclusion

In conclusion, compound **1** with terminal Lys amino acid group linked to NBD fluorophore by triazole ring was successfully applied in selective recognition of Hg^{2+} in aqueous solution. In the presence of Hg^{2+}, remarkable fluorescence quenching of **1** was observed. Meanwhile a red shift was obtained both in absorption and fluorescence spectra, which was utilized for naked-eye detection of Hg^{2+}. Other metal ions examined show almost no influence on spectral properties of **1** in aqueous solution. Control experiments by using more rigid compound **2** demonstrated the importance of cooperative binding ability of amino acid group in improving the sensitivity of sensing system, allowing wide structural diversity of molecular sensory platforms based on triazole group. Furthermore, ^1H NMR titration was performed to get insight into the complexation mode of **1** to Hg^{2+}, which verified the role of triazole group to the spectral change.

Acknowledgements

YBR thanks the China Scholarship Council (CSC) for support through a scholarship to work at PPSM, Institut d'Alembert, ENS Cachan.

Appendix. Supplementary data

Supplementary data associated with this article can be found in the online version, at doi:10.1016/j.dyepig.2011.01.004.

References

[1] (a) Vallee BL, Ulmer DD. Biochemical effects of mercury, cadmium, and lead. Annual Review of Biochemistry 1972;41:91–128;
(b) Gutknecht J. Inorganic mercury (Hg^{2+}) transport through lipid bilayermembranes. Journal of Membrane Biology 1981;61:61–6.

[2] Nolan EM, Lippard SJ. Tools and tactics for the optical detection of mercuric ion. Chemical Reviews 2008;108:3443–80.

[3] (a) Kim HN, Lee MH, Kim HJ, Kim JS, Yoon J. A new trend in rhodamine-based chemosensors: application of spirolactam ring-opening to sensing ions. Chemical Society Reviews 2008;37:1465–72;
(b) Liu B, Tian H. A selective fluorescent ratiometric chemodosimeter for mercury ion. Chemical Communications; 2005:3156–8;

(c) Yoon S, Miller EW, He Q, Do PH, Chang CJ. A bright and specific fluorescent sensor for mercury in water, cells, and tissue. Angewandte Chemie-International Edition 2007;46:6658–61;
(d) Zhang XL, Xiao Y, Qian XH. A ratiometric fluorescent probe based on FRET for imaging Hg^{2+} ions in living cells. Angewandte Chemie-International Edition 2008;47:8025–9;
(e) Liu L, Zhang GX, Xiang JF, Zhang DQ, Zhu DB. Fluorescence “turn on” chemosensors for Ag^{+} and Hg^{2+} based on tetraphenylethylene motif featuring adenine and thymine moieties. Organic Letters 2008;10:4581–4;
(f) Zhu M, Yuan MJ, Liu XF, Xu JL, Lv J, Huang CS, et al. Visible near-infrared chemosensor for mercury ion. Organic Letters 2008;10:1481–4;
(g) Yan YE, Hu Y, Zhao GP, Kou XM. A novel azathia-crown ether dye chromogenic chemosensor for the selective detection of mercury(II) ion. Dyes and Pigments 2008;79:210–5;
(h) Zou Q, Tian H. Chemodosimeters for mercury(II) and methylmercury(I) based on 2,1,3-benzothiadiazole. Sensors and Actuators B-Chemical 2010;149:20–7;
(i) Leng B, Jiang JB, Tian H. A mesoporous silica supported Hg^{2+} chemodosimeter. AIChE Journal 2010;56:2957–64;
(j) Guo ZQ, Zhu WH, Zhu MM, Wu XM, Tian H. Near-Infrared cell-permeable Hg^{2+}-selective ratiometric fluorescent chemodosimeters and fast indicator paper for MeHg^{+} based on tricarbocyanines. Chemistry-A European Journal 2010;16:14424–32.

[4] (a) Ono A, Togashi H. Highly selective oligonucleotide-based sensor for mercury(II) in aqueous solutions. Angewandte Chemie-International Edition 2004;43:4300–2;
(b) Liu J, Lu Y. Rational design of “turn-on” allosteric DNAzyme catalytic beacons for aqueous mercury ions with ultrahigh sensitivity and selectivity. Angewandte Chemie-International Edition 2007;46:7587–90;
(c) Hollenstein M, Hipolito C, Lam C, Dietrich D, Perrin DM. A highly selective DNAzyme sensor for mercuric ions. Angewandte Chemie-International Edition 2008;47:4346–50;
(d) Li T, Li BL, Wang EK, Dong SJ. G-quadruplex-based DNAzyme for sensitive mercury detection with the naked eye. Chemical Communications; 2009:3551–3;
(e) Gao XY, Xing GM, Yang YL, Shi XL, Liu R, Chu WG, et al. Detection of trace Hg^{2+} via induced circular dichroism of DNA wrapped around single-walled carbon nanotubes. Journal of the American Chemical Society 2008;130:9190–1.

[5] (a) Lee JS, Han MS, Mirkin CA. Colorimetric detection of mercuric ion (Hg^{2+}) in aqueous media using DNA-functionalized gold nanoparticles. Angewandte Chemie-International Edition 2007;46:4093–6;
(b) Huang CC, Yang Z, Lee KH, Chang HT. Synthesis of highly fluorescent gold nanoparticles for sensing mercury(II). Angewandte Chemie-International Edition 2007;46:6824–8;
(c) Xue XJ, Wang F, Liu XG. One-step, room temperature, colorimetric detection of mercury (Hg^{2+}) using DNA/nanoparticle conjugates. Journal of the American Chemical Society 2008;130:3244–5;
(d) Darbha GK, Singh AK, Rai US, Yu E, Yu HT, Ray PC. Selective detection of mercury (II) ion using nonlinear optical properties of gold nanoparticles. Journal of the American Chemical Society 2008;130:8038–43;
(e) Xie JP, Zheng YG, Ying JY. Highly selective and ultrasensitive detection of Hg^{2+} based on fluorescence quenching of Au nanoclusters by Hg^{2+}-Au^{+} interactions. Chemical Communications 2010;46:961–3.

[6] (a) White BR, Liljestrand HM, Holcombe JA. A ‘turn-on’ FRET peptide sensor based on the mercury binding protein MerP. Analyst 2008;133:65–70;
(b) Chen P, He C. A general strategy to convert the MerR family proteins into highly sensitive and selective fluorescent biosensors for metal ions. Journal of the American Chemical Society 2004;126:728–9;
(c) Wegner SV, Okesli A, Chen P, He C. Design of an emission ratiometric biosensor from MerR family proteins: a sensitive and selective sensor for Hg^{2+}. Journal of the American Chemical Society 2007;129:3474–5.

[7] (a) Kim IB, Bunz UHF. Modulating the sensory response of a conjugated polymer by proteins: an agglutination assay for mercury ions in water. Journal of the American Chemical Society 2006;128:2818–9;
(b) Ren XS, Xu QH. Highly sensitive and selective detection of mercury ions by using oligonucleotides, DNA intercalators, and conjugated polymers. Langmuir 2009;25:29–31;
(c) Liu XF, Tang YL, Wang LH, Zhang J, Song SP, Fan CH, et al. Optical detection of mercury(II) in aqueous solutions by using conjugated polymers and label-free oligonucleotides. Advanced Materials 2007;19:1471–4.

[8] (a) Hawker CJ, Wooley KL. The convergence of synthetic organic and polymer chemistries. Science 2005;309:1200–5;
(b) Kolb HC, Sharpless KB. The growing impact of click chemistry on drug discovery. Drug Discovery Today 2003;8:1128–37;
(c) Meldal M, Tornoe CW. Cu-catalyzed azide-alkyne cycloaddition. Chemical Reviews 2008;108:2952–3015;
(d) Moses JE, Moorhouse AD. The growing applications of click chemistry. Chemical Society Reviews 2007;36:1249–62.

[9] Li YJ, Huffman JC, Flood AH. Can terdentate 2,6-bis(1,2,3-triazol-4-yl) pyridines form stable coordination compounds? Chemical Communications; 2007:2692–4.

[10] (a) Hung HC, Cheng CW, Wang YY, Chen YJ, Chung WS. Highly selective fluorescent sensors for Hg^{2+} and Ag^{+} based on bis-triazole-coupled polyoxyethylenes in MeOH solution. European Journal of Organic Chemistry; 2009:6360–6;
(b) Nguyen DM, Frazer A, Rodriguez L, Belfield KD. Selective fluorescence sensing of zinc and mercury ions with hydrophilic 1,2,3-triazolyl fluorene probes. Chemistry of Materials 2010;22:3472–81;
(c) Kumar A, Pandey PS. Steroidal 1,2,3-triazole-based sensors for Hg^{2+} ion and their logic gate behaviour. Tetrahedron Letters 2009;50:5842–5;
(d) Maity D, Govindaraju T. Pyrrolidine constrained bipyridyl-dansyl click fluoroionophore as selective Al^{3+} sensor. Chemical Communications 2010;46:4499–501;
(e) Kim SH, Choi HS, Kim J, Lee SJ, Quang DT, Kim JS. Novel optical/electrochemical selective 1,2,3-triazole ring-appended chemosensor for the Al^{3+} ion. Organic Letters 2010;12:560–3;
(f) Brombosz SM, Appleton AL, Zappas AJ, Bunz UHF. Water-soluble benzo- and naphtho-thiadiazole-based bistriazoles and their metal-binding properties. Chemical Communications 2010;46:1419–21;
(g) Varazo K, Xie F, Gulledge D, Wang Q. Synthesis of triazolyl anthracene as a selective fluorescent chemosensor for the Cu(II) ion. Tetrahedron Letters 2008;49:5293–6;
(h) Schweinfurth D, Hardcastle KI, Bunz UHF. 1,3-Dipolar cycloaddition of alkynes to azides. Construction of operationally functional metal responsive fluorophores. Chemical Communicatioins; 2008:2203–5;
(i) Chang KC, Su IH, Senthilvelan A, Chung WS. Triazole-modified calix[4] crown as a novel fluorescent on-off switchable chemosensor. Organic Letters 2007;9:3363–6;
(j) Park SY, Yoon JH, Hong CS, Souane R, Kim JS, Matthews SE, et al. A pyrenyl-appended triazole-based calix[4]arene as a fluorescent sensor for Cd^{2+} and Zn^{2+}. Journal of Organic Chemistry 2008;73:8212–8;
(k) Tamanini E, Flavin K, Motevalli M, Piperno S, Gheber LA, Todd MH, et al. Cyclam-based “clickates”: homogeneous and heterogeneous fluorescent sensors for Zn(II). Inorganic Chemistry 2010;49:3789–800;
(l) Colasson B, Save M, Milko P, Roithova J, Schroder D, Reinaud O. A ditopic calix[6]arene ligand with N-methylimidazole and 1,2,3-triazole substituents: synthesis and coordination with Zn(II) cations. Organic Letters 2007;9:4987–90;
(m) Huang S, Clark RJ, Zhu L. Highly sensitive fluorescent probes for zinc ion based on triazolyl-containing tetradentate coordination motifs. Organic Letters 2007;9:4999–5002;
(n) David O, Maisonneuve S, Xie J. Generation of new fluorophore by Click chemistry: synthesis and properties of beta-cyclodextrin substituted by 2-pyridyl triazole. Tetrahedron Letters 2007;48:6527–30;
(o) Souchon V, Maisonneuve S, David O, Leray I, Xie J, Valeur B. Photophysics of cyclic multichromophoric systems on β-cyclodextrin and calix[4]arene with appended pyridin-2’-yl-1,2,3-triazloe groups. Photochemical Photobiological Sciences 2008;7:1323–31;
(p) Maisonneuve S, Fang Q, Xie J. Benzothiadiazoyl-triazoyl cyclodextrin: a selective fluoroionophore for Ni(II). Tetrahedron 2008;64:8716–20;
(q) Ruan YB, Maisonneuve S, Li C, Tang J, Xie J. Cooperative recognition of Cu^{2+} based on amino acids tethered benzothiadiazoyl-bistriazoles. Frontiers of Chemistry in China 2010;5:208–13;
(r) Garcia L, Maisonneuve S, Xie J, Guillot R, Dorlet P, Rivière E, et al. Sugars to control ligand shape in metal complexes: conformationally constrained glycoligands with a predetermination of stereochemistry and a structural control. Inorganic Chemistry 2010;49:7282–8.

[11] Stuchbury T, Shipton M, Norris R, Malthouse JPG, Brocklehurst K, Herbert JAL, et al. Reporter group delivery system with both absolute and selective specificity for thiol-groups and an improved fluorescent-probe containing 7-nitrobenzo-2-oxa-1,3-diazole moiety. Biochemical Journal 1975;151:417–32.

[12] (a) Jiang W, Fu QQ, Fan HY, Wang W. An NBD fluorophore-based sensitive and selective fluorescent probe for zinc ion. Chemical Communications; 2008:259–61;
(b) Ramachandram B, Samanta A. Transition metal ion induced fluorescence enhancement of 4-(N, N-dimethylethylenediamino)-7-nitrobenz-2-oxa-1,3-diazole. Journal of Physical Chemistry A 1998;102:10579–87;
(c) Kim SH, Kim JS, Park SM, Chang SK. Hg^{2+}-selective OFF-ON and Cu^{2+}-selective ON-OFF type fluoroionophore based upon cyclam. Organic Letters 2006;8:371–4;
(d) Xu ZC, Kim GH, Han SJ, Jou MJ, Lee C, Shin I, et al. An NBD-based colorimetric and fluorescent chemosensor for Zn^{2+} and its use for detection of intracellular zinc ions. Tetrahedron 2009;65:2307–12;
(e) Qian F, Zhang CL, Zhang YM, He WJ, Gao X, Hu P, et al. Visible light excitable Zn^{2+} fluorescent sensor derived from an intramolecular charge transfer fluorophore and its in vitro and in vivo application. Journal of the American Chemical Society 2009;131:1460–8.

[13] Li C, Henry E, Mani NK, Tang J, Brochon JC, Deprez E, et al. Click chemistry to fluorescent amino esters: synthesis and spectroscopic studies. European Journal of Organic Chemistry; 2010:2395–405.